Renewable Energy 202 (2023) 554–565

Contents lists available at ScienceDirect

Renewable Energy

journal homepage: www.elsevier.com/locate/renene

Sizing of hybrid microgrids considering life cycle assessment

Iván Jiménez-Vargas *, Juan M. Rey, German Osma-Pinto

Escuela de Ingenierías Eléctrica, Electrónica y de Telecomunicaciones, Universidad Industrial de Santander, Bucaramanga 680002, Colombia

ARTICLE INFO

Keywords:
Life cycle assessment
Microgrids
Multi-objective optimization
Renewable energies

ABSTRACT

The sizing of microgrids consists of determining the capacity of its main elements, ensuring financial, technical, reliability and environmental criteria. However, regarding the environmental impact, most of the literature addresses this evaluation by exclusively quantifying the emissions in the microgrid operation stage, which tends to underestimate the life cycle ecological cost of the microgrid's elements. In this sense, this paper proposes a sizing approach that integrates the life cycle assessment of the implementation and operation stages by adapting a multi-objective function inspired by the well-known life cycle assessment methodology called ReCiPe. For this purpose, information from several sources was compiled and adapted to quantify different environmental impacts in the sizing formulation. A case study of a solar/wind/battery/diesel microgrid is presented, showing that calculating the environmental impact indicators considering only emissions in the operation leads to a value 54.60% lower than the proposed approach. It was also found that the underestimation of environmental indicators can lead to a selection of a more polluting microgrid sizing configuration, which remarks the relevance of an adequate environmental evaluation in the sizing procedure.

1. Introduction

Some prospective energy studies indicate that by 2040 more than 70% of energy will be produced by fossil sources [1], while the share of fossil fuels is estimated at 80% to 90% [2]. This scenario will cause an increase in greenhouse gas (GHG) emissions to historical maximums [3]. In this context, the solutions that allow energy generation with reduced GHG emissions and other environmental impacts are decisive for sustainable development, such as renewable energies and electrical microgrids (MG).

An MG is an electrical network that contains renewable and non-renewable distributed energy resources (DERs), energy storage systems (ESSs), communications and control devices capable of supplying local demand without using transmission networks [4,5]. This type of network is an alternative to traditional power systems and is considered a greener option due to the use of renewable energies [6,7]. However, MGs have some operational and cost disadvantages compared to conventional distribution networks, among which the high initial investment costs stand out. This concern is the main focus of the MGs sizing problem [8,9].

The sizing of MGs consists of determining the capacity of the MG's DERs and ESSs according to single or multiple optimization criteria [10]. Sizing MGs can become a challenging task since the integration of DERs and ESSs depend on several factors, such as climatic conditions and load variability, making the nature of the problem non-deterministic [11]. Without suitable techniques, MGs tend to be undersized or with high amounts of wasted energy. This problem usually includes objectives, dispatch rules, and restrictions on the system's future operation. Optimizing the MG design goals can be financial, technical, social, environmental, or a combination [10]. This problem can be formulated and solved using optimization software such as GAMS, AMPL, and Matlab, or specialized simulation software such as HOMER Pro [12], HYBRID2 [13], and iHOGA [14].

In the literature, there is abundant material on optimal sizing [15,16]. Authors have focused mainly on analyzing the use of algorithms to improve the run-time and accuracy of the solutions [17], or have studied the impact of considering the stochastic behavior of the load and the generation [18], as well as the inclusion of complex load prediction models [19], demographic factors [20] and environmental indicators.

Regarding this last aspect, several studies have evaluated the environmental component of MG sizing [21–23]. Most of these works address the problem by quantifying the pollutants' emissions. However, although renewable generation or batteries do not emit GHG in their operation, these systems' life cycle (LC) has an important ecological cost that must be considered [24,25]. This issue is studied in depth in the works that focus on assessing the environmental impact of hybrid energy systems operation and planning using Life Cycle Assessment (LCA), a technique for analyzing the environmental

* Corresponding author.
E-mail address: ivan.jimenez@correo.uis.edu.co (I. Jiménez-Vargas).

https://doi.org/10.1016/j.renene.2022.11.103
Received 25 May 2022; Received in revised form 1 November 2022; Accepted 22 November 2022
Available online 25 November 2022

Nomenclature

Acronyms

AP	Acidification Potential
$BESS$	Battery Energy Storage System
DER	Distributed Energy Resources
DG	Diesel Generator
EMS	Energy Management Strategy
EP	Eutrophication Potential
ESS	Energy Storage System
ET	Ecotoxicity
$FAET$	Freshwater Aquatic Ecotoxicity
FEP	Freshwater Eutrophication Potential
GHG	Greenhouse Gases
GWP	Global Warming Potential
LC	Life Cycle
LCA	Life Cycle Assessment
$MAET$	Marine Aquatic Ecotoxicity Potential
MEP	Marine Eutrophication Potential
MG	Microgrid
NCM	Nickel Cobalt Manganese Oxide
$NMVOC$	Non-methane volatile organic compounds
NPC	Net Present Cost
POF	Photochemical Ozone formation
PV	Photovoltaic
TET	Terrestrial Ecotoxicity Potential
WT	Wind Turbine

Variables

η	Efficiency
A	Area
AG	Annual Generation
C_{in}	Lower Cutting Speed
C_{out}	Upper Cutting Speed
CF	Characterization Factor
CP	Capital Price
DE	Degradation of DERs
E	Energy
EcS	Economic Solution
EI	Environmental Impact
EnS	Environmental Solution
ESI	Ecosystem Impact
ETP	Energy Throughout
F	Cash Flow of Costs
FC	Fuel Consumption
GE	Guaranteed Energy of DG
I	Solar Irradiance
i	Real Discount Rate
IE	Insufficient Energy
$LPSP$	Loss of Power Supply Probability
N	Quantity of DERs
NC	Nominal Capacity
OH	Operation Hours
OM	Operation and Maintenance Cost
P	Power
SOC	State of Charge
t	Time Period
T_c	Operating Temperate
TEL	Total Energy Lost
ul	Useful Lifetime
V	Wind Velocity

Index

a	Protection Area
c	Cultural Perspective
d	Diesel fuel
e	Endpoint
f	Diesel Consumption
G	Set of DERs
IC	Initial Capital
L	Load
m	Midpoint
$M \rightarrow E$	Midpoint to Endpoint Transformation
OM	Operation and Maintenance
R	Rated
RE	Replacement
SA	Salvage
x	Stressors
y	Years

impacts associated with a product over its life cycle [26–28]. Only a few studies use LCA methodologies integrated into the sizing formulation [12,29,30]. However, this is performed by analyzing only the MG operation and neglecting the previous stages, such as manufacturing and implementation, so the total environmental evaluation tends to be underestimated.

In Refs. [31,32] are presented proposals that partially consider LCA in the optimal sizing formulation. In Ref. [31], the LCA analysis is reduced to assume a typical day during the evaluation period to mitigate the environmental impact of using diesel generators, while Ref. [32] presents a sizing approach with an LC indicator based exclusively on the energy embodied in the MG components. Moreover, Ref. [33] presents a sizing of a photovoltaic (PV) MG, including an LCA, to compare environmental impacts by each element. In this case, the environmental assessment is not integrated into the problem formulation but is done to a specific sizing solution. Thus, the absence of studies that analyze the sizing considering LCA in the main stages of an MG design is identified.

Motivated by this research challenge, this paper proposes an MG sizing approach that integrates the LCA in the formulation by adapting a multi-objective function. This proposed approach allows evaluation of the implementation and operation stages following the internationally well-known LCA methodology called ReCiPe. For this purpose, the information from several sources was compiled and adapted to quantify different LC impacts, avoiding underestimating the environmental evaluation of the components of the MG.

The rest of the paper is organized as follows: Section 2 presents the methodology. Section 3 presents the formulation of the LCA-based objective function. Section 4 shows the modeling of the components and the economic function. In Section 5, the simulations and analysis of the results are carried out. Finally, the conclusions are presented in Section 6.

2. Methodology

Fig. 1 presents a graphical abstract of the contribution of this paper. As mentioned above, common MG sizing approaches to address the quantification of environmental impacts by exclusively calculating the

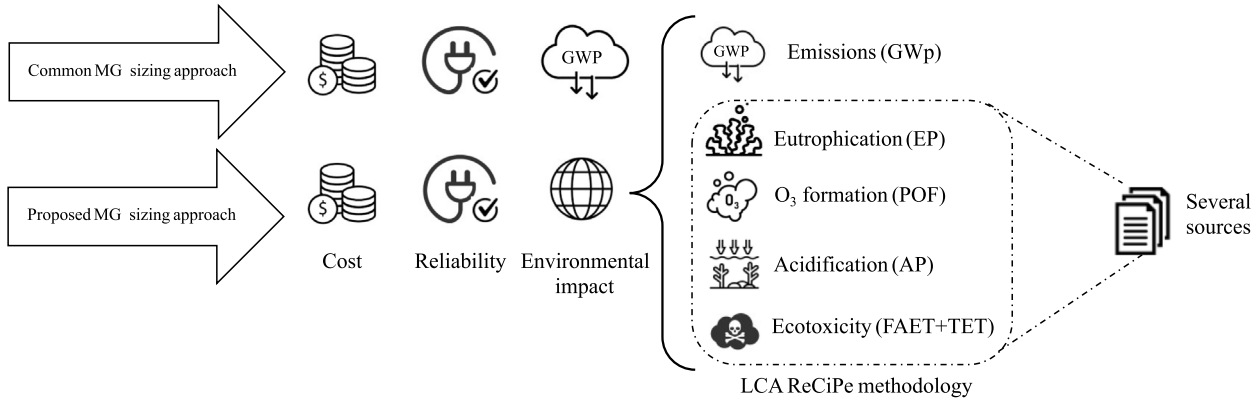

Fig. 1. Graphical abstract.

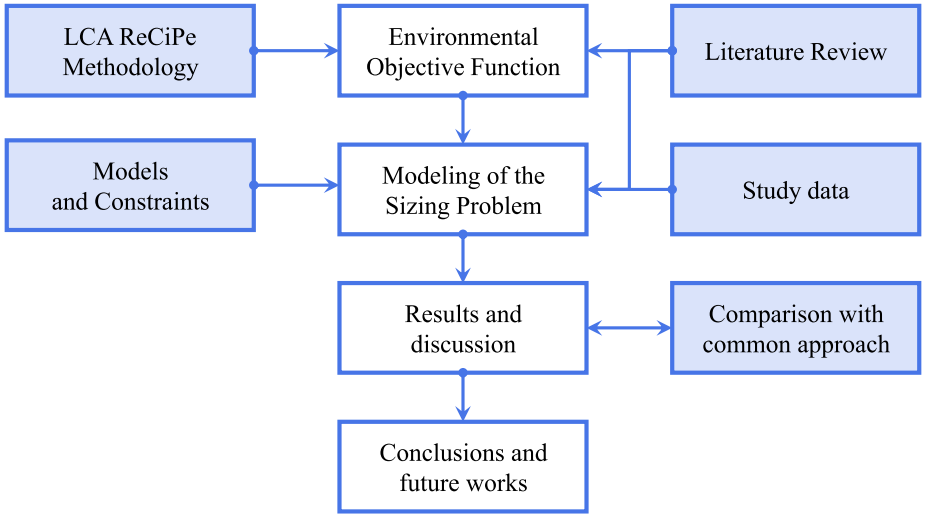

Fig. 2. Research flow chart.

emissions of pollutants. The proposed MG sizing approach, inspired by LCA ReCiPe methodology, adds other indicators in order to integrate the implementation and operation stages in the environmental impact assessment. The information to calculate the parameters is obtained from many sources through a bibliographic search.

The methodology followed for this manuscript is presented as a flow chart in Fig. 2. First, the environmental objective function is formulated by adapting the LCA ReCiPe methodology. As this methodology is proposed for any product or service, a literature review is performed to find and adapt the parameters of the environmental factors used in the calculation of the environmental impact. Then, the modeling of the sizing problem is presented, detailing the equations that describe the power injection and storage. Also, the study data is presented, including the load profile, the primary energy resources, and the values of the economic and technical parameters. Next, the results and discussion are presented. First, the simulations of the proposed approach are compared with a common sizing approach that only considers the GWP impact. Then, the environmental component of the Pareto front solutions is analyzed. Finally, the main finding of the paper is concluded, and some future work lines are proposed.

3. Environmental objective function

The LCA is a technique for evaluating the environmental impacts associated with the supply chain, that is, from raw material extraction to its final disposal [34]. This technique aims to analyze the performance of products or services; however, in this work, some of the main characteristics of an LCA are adapted to be used as a tool for the sizing of an MG by formulating an objective function. This section presents the methodology in which this function was inspired and the environmental impact indicators associated.

3.1. ReCiPe v1.1

ReCiPe methodology is an effort to harmonize LCA, as well as to provide tools, data, relationships, and categories that allow the quantification of the environmental impact of a product or service through a series of factors that relate to the amounts of polluting material emitted with midpoint and endpoint environmental impacts [35]. The method got its name from the initials of the creator institutes (RIVM and Radboud University, CML, and PRé Consultants) since it provides a “recipe” to calculate LC impact. The main idea behind the ReCiPe method is to transform the emissions of certain substances (stressors) into a limited number of environmental impact indicators through a series of characterization factors.

These factors are *midpoint* when they are directly associated with the emissions of a stressor, while they are *endpoint* when they are associated with any of these three protected areas: human health, ecosystem quality, and resource scarcity. Specific stressors are associated with one or more areas of protection. Fig. 3 presents the relationship between the midpoint impact categories and the protected areas.

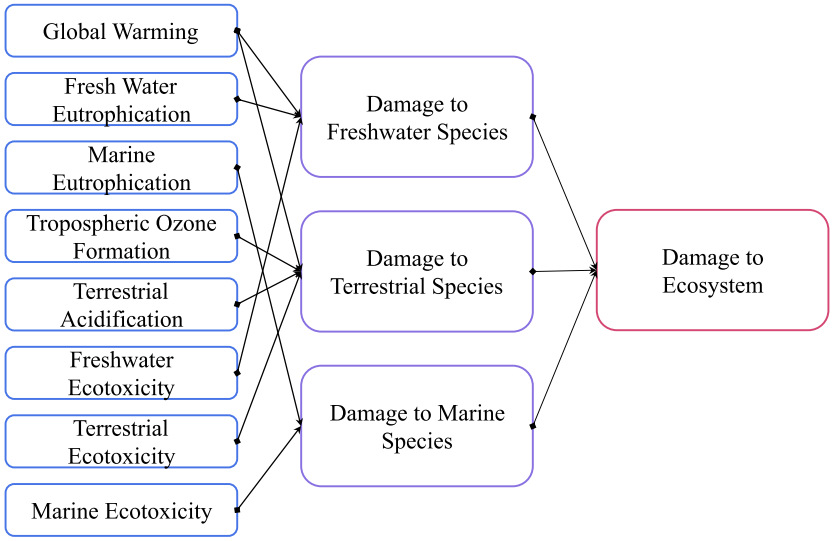

Fig. 3. Impact categories and their relationship with the protection areas covered by the ReCiPe.
Source: Adapted from [35].

Table 1
Environmental impact indicators of 1 kWh of PV energy.

Category	Indicator	Value
Global warming	GWP	1e−1 kg CO_2e
Eutrophication	EP	1e−4 kg PO_4^{-3}e
O_3 formation	POF	1e−4 kg C_2H_4e
Acidification	AP	4e−4 kg SO_2e
Ecotoxicity	FAET	2e−2 kg 1,4-DBe
	TET	2e−14 kg 1,4-DBe

Table 2
Environmental impact for each kWh of the capacity of lithium batteries type NCM.

Category	Indicator	Value
Global warming	GWP	93.57 kg CO_2e
Eutrophication	F-EP	0.01 kg Pe
	M-EP	0.02 kg Ne
O_3 formation	POF	0.29 kg NMVOCe
Acidification	AP	0.49 kg SO_2e
Ecotoxicity	FAET	1.5 kg 1,4-DBe
	TET	0.01 kg 1,4-DBe

3.2. Environmental impact indicators

According to Fig. 3, the protection area called Damage to Ecosystems is associated with three impact paths: Damage to Freshwater Species, Damage to Terrestrial Species, and Damage to Marine Species. This model proposes to quantify the impact on these three groups of species by determining the emissions of stressors associated with global warming, water use, ecotoxicity, eutrophication, ozone formation, and acidification. Likewise, each impact has an associated unit of measure, given the amount emitted from the stressor.

There are no harmonized studies that collect the environmental impact of each technology in all categories; in fact, the availability of generalizable information is one of the main drawbacks when dealing with LCA. For this reason, different LCA studies were reviewed to compile and adapt the emissions of each stressor for each kWh generated and, thus, establish a relationship between energy production and emissions.

3.2.1. Environmental impact of photovoltaic systems

For the PV system, the information was taken from Ref. [36]. Through a harmonization process and following the LCA CML 2000 methodology, the authors estimated the environmental impact of generating 1 kWh. Table 1 collects the data reported for the five categories of interest. Note that the Ecotoxicity (ET) impact is divided into Freshwater Ecotoxicity (FAET) and Terrestrial Ecotoxicity (TET).

3.2.2. Environmental impact of wind turbines

The values of the indicators for wind turbines (WT) were compiled from different sources since there is no work that reports complete information. For GWP, EP, and AP indicators, data in Ref. [37] was used, in which a fitting curve relates the WT nominal capacity as follows:

$$GWP_{wt} = 2615.6 \times NC_{wt}^{0.7462} \text{ kg } CO_2\text{e} \quad (1)$$

$$EP_{wt} = 2.562 \times NC_{wt}^{0.7418} \text{ kg } PO_4^{-3}\text{e} \quad (2)$$

$$AP_{wt} = 16.472 \times NC_{wt}^{0.7385} \text{ kg } SO_2\text{e} \quad (3)$$

where, NC_{wt} represents the nominal capacity of the WT in kW. For POF and ET, the data for small WT in Ref. [38] was considered, i.e. 1.72×10^{-4} kg NO_xe for POF, 1.60×10^{-4} kg 1,4-DBe for TET, and 0.01 kg 1,4-DBe for FAET.

3.2.3. Environmental impact of battery systems

For battery energy storage systems (BESS), a type NCM (nickel cobalt manganese oxide) lithium-ion batteries was assumed, as they are popular in static power generation and backup power systems [39]. The data was taken from the ReCiPe-based LCA performed in Ref. [40]. The data reported per kWh of the capacity of the NCM batteries are collected in Table 2.

3.2.4. Environmental impact of diesel generation

The environmental impact of diesel generation (DG) is concentrated almost 95% in the emissions derived from its operation [41]. In this case, only the reports of emissions per liter of diesel fuel consumed and the impact of its burning are collected. For this, the work in Ref. [42] was used to obtain information on GWP, while the website of the Government of Canada was used for information regarding AP and POF [43]. No information was identified on EP and ET. Table 3 collects the information for DG emissions.

Table 3
Environmental impact per liter of diesel consumed.

Category	Indicator	Value
Global warming	GWP	2.81 kg CO_2e
O_3 formation	POF	7.24e−2 kg NMVOCe
Acidification	AP	4.80e−3 kg SO_2e

Table 4
Values of the transformation factors from midpoint to endpoint.

Indicator	Value	Units
GWP	2.8e−9	species-year/kg CO_2e
FEP	6.1e−7	species-year/kg Pe
MEP	1.7e−9	species-year/kg Ne
POF	1.3e−7	species-year/kg NO_xe
AP	2.1e−7	species-year/kg SO_2e
FAET	7.0e−10	
MAET	1.1e−10	species-year/1,4DCBe
TET	5.4e−8	

3.3. Objective function

In this section, the environmental objective function is formulated. It is necessary to relate the environmental impacts with the nominal capacity of the DERs or their energy production. Likewise, the environmental objective function formulated must include the five categories in the same units. In the case of the relationship between impacts and nominal capacity, it was chosen to do so using energy production; that is, the environmental impact is quantified per kWh of DERs, except for DG, which was quantified per liter since it is practical for implementing the sizing problem formulation.

Regarding the dimensional analysis of the objective function, ReCiPe allows transforming the indicators from midpoint to endpoint through some factors. For example, for the ecosystem damage protection area, all midpoint indicators can be transformed to the time-integrated species loss — TISL indicator, measured in species-year. The transformation is done by multiplying the environmental impact by a midpoint-to-endpoint transformation factor. This can be expressed as:

$$CF_{e_{x,c,a}} = CF_{m_{x,c}} \times F_{M\to E_{c,a}} \tag{4}$$

where, CF_e represents the endpoint characterization factor, CF_m the midpoint impact characterization factor and $F_{M\to E}$ represents the transformation factor. The subscripts x, c, and a denote the stressor of interest, the cultural perspective and the protection area, respectively. The value of the transformation factor for each category is shown in Table 4. Note that F-EP refers to Freshwater EP and M-EP refers to Marine EP.

An essential aspect of LCA methodologies is that they depend on the cultural perspective adopted, influencing the stated assumptions for constructing the models. ReCiPe handles three cultural perspectives: individualistic, hierarchical, and egalitarian. The perspective affects the transformation factor values, so it is imperative to choose one. For this work, the hierarchical perspective was adopted considering the time horizon on which the environmental impact operates (100 years) and the useful life of the MG. From the preceding information, the objective function is formulated following this procedure:

1. All environmental impacts are expressed in the units proposed by ReCiPe for each category.
2. Environmental impacts are expressed per kWh or L.
3. Each environmental impact is multiplied by the design variable of the problem, that is, by the power generated (for WT, FV and BESS) or diesel consumption (for DG).
4. The resulting term is multiplied by the corresponding transformation factor.
5. All the terms are added to obtain a linear function.

Table 5
Values for calculating the coefficient of the environmental impact function for PV.

Indicator	CF_m	$F_{M\to E}$	CF_e
GWP	1.0e−1	2.8e−9	2.8e−10
FEP	3.3e−5	6.1e−7	2.0e−11
POF	4.8e−6	1.3e−7	6.2e−13
AP	4.0e−4	2.1e−7	8.4e−11
FAET	2.0e−2	7.0e−10	1.4e−11
TET	2.0e−14	5.4e−8	1.1e−21
$\sum CF_e$			3.99e−10

Next, this procedure is applied to each DER. For example, the data reported in Tables 1 and 4 is used to obtain the objective function component corresponding to the impact of the production of 1 kWh of PV energy. The values of Table 1 for EP and O_3 Formation must be transformed to the ReCiPe units since they are given in units of the CML 2000 methodology. It is possible to do this thanks to the data in Ref. [44].

Note that all emissions related to eutrophication reported in Ref. [36] were assumed in the F-EP indicator for simplicity since there is no information on what proportion of the substance is emitted in seawater. By converting the corresponding data from Table 1 and multiplying them by the factors from Table 4, the impact coefficient of PV can be obtained, as shown in Table 5.

Therefore, the impact coefficient of generating 1 kWh of energy with PV is 3.99×10^{-10} species-year. Thus, the linear function of the environmental impact of PV is

$$IA_{PV} = 3.99 \times 10^{-10} E_{PV} \tag{5}$$

where, IA_{PV} represents the environmental impact of electricity generation in species-year and E_{PV} represents the energy generated by the PV in kWh.

A similar procedure is applied to the remain DERs taking into account the following considerations: for the WT, the indicators of GWP, EP, and AP are presented in terms of the nominal capacity; for the BESS, the data reported in Table 2 refers to the impact per kWh of capacity. The impacts were transformed in terms of the energy produced through the division of the total impact by the energy generated in the useful life as follows:

$$GWP^*_{WT} = \frac{GWP_{wt}}{vu_{WT} \times AG_{WT}} \tag{6}$$

$$EP^*_{WT} = \frac{EP_{wt}}{vu_{WT} \times AG_{WT}} \tag{7}$$

$$AP^*_{WT} = \frac{AP_{wt}}{vu_{WT} \times AG_{WT}} \tag{8}$$

where, GWP^*_{WT} is the GWP in kgCO_2e/kWh, EP^*_{WT} is the EP in kg $PO_4{}^{-3}$e/kWh, AP^*_{WT} is the AP in kgSO2e/kWh, vu_{WT} is the useful life of the WT in years and AG_{WT} is the annual generation of the turbines. This transformation depends on the technical specifications of the turbine, so numerical values can only be obtained if a specific model is defined. For this work, a 10 kW turbine from the Aeolos brand was used as a study case, with a useful lifetime of 20 years. Thus, the energy generated in the useful life given the wind profile of the location of interest (see Section 4) is:

$$vu_{WT} AG_{WT} = 20 \times 2.43 \times 10^4 = 486 \text{ MWh} \tag{9}$$

Thus, the environmental impact in the damage to ecosystems produced by generating 1 kWh with the WT would be estimated as follows:

$$IA_{WT} = 1.67 \times 10^{-10} E_{WT} \tag{10}$$

In the case of BESS, the same procedure was used and the impact was transformed using the energy throughput of the selected battery. The conversion is done as follows

$$IA^*_{BESS} = IA_{BESS} \times \frac{NC_{BESS}}{ETP_{BESS}} \tag{11}$$

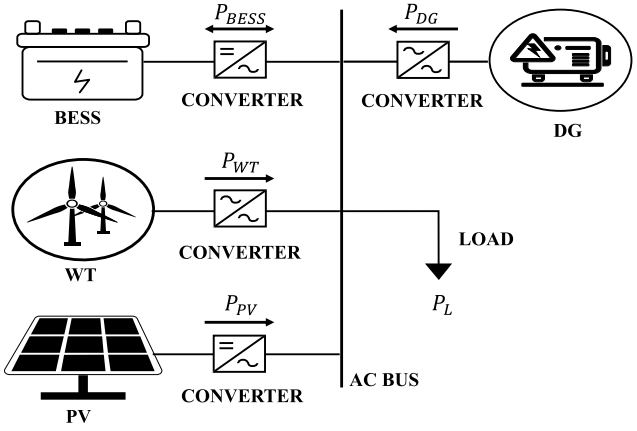

Fig. 4. Configuration of the microgrid for the study case.

where, IA^*_{BESS} indicates the environmental impact per kWh generated, IA_{BESS} is the environmental impact per kWh of capacity, NC_{BESS} is the nominal capacity of the battery and ETP_{BESS} is the energy throughout of the battery. The type of battery selected is A 9.8 kWh unit and its ETP is 30 MWh. Therefore, the expression to quantify the environmental impact of the BESS in terms of its energy flow is

$$IA_{BESS} = 1.3 \times 10^{-10} \left| E_{BS} \right| \tag{12}$$

Finally, for the DG, the only modification regarding the values in Table 3 is that the POF is given in kg NMVOC$-eq$, but ReCiPe suggests using kg $NO_x - eq$. The transformation factor of these units is 0.29, according to ReCiPe. The linear expression to quantify the impact of emissions from diesel-burning as a function of diesel consumption f_{DG} is:

$$IA_{DG} = 1.83 \times 10^{-8} f_{DG} \tag{13}$$

Then, the objective function is constructed from the sum of the of expressions (5), (10), (12) and (13):

$$\begin{aligned} IA_{MG} = {} & 3.98 \times 10^{-10} E_{PV} + 1.67 \times 10^{-10} E_{WT} \\ & + 1.25 \times 10^{-10} \left| E_{BS} \right| + 1.83 \times 10^{-8} f_{DG} \end{aligned} \tag{14}$$

4. Modeling of the sizing problem

This section presents the considerations and mathematical models for the sizing formulation. The MG corresponds to a PV/WT/DG/BESS system (see Fig. 4) due to this configuration has a good relationship between reliability and economy [45]. The objectives are to reduce the net present cost (NPC) and the LC emissions considering ReCiPe. A rule-based energy management strategy (EMS) was chosen for a five-year horizon. The procedure followed for the modeling is based on methodologies used multiple times in recent literature [16,17].

4.1. Economic objective function

The economic indicator chosen as the objective was the NPC since it allows to the transformation of the money flows from future years to their equivalent value in the current currency.

$$NPC = C_{IC} + C_{OM} + C_{FC} + C_{RE} + C_{SA} \tag{15}$$

where, C_{IC} is the initial capital, C_{OM} is the operation and maintenance (O&M) costs, C_{FC} is the fuel consumption costs, C_{RE} is the replacement costs, and C_{SA} is the salvage of the equipment at the end of the lifetime. The annual costs were calculated as follows:

$$C_{IC_y} = \sum_G N_G CP_G \tag{16}$$

$$C_{OM_y} = N_{DG} OM_{DG} OH_{DG} + \sum_{G \neq DG} (N_G OM_G) \tag{17}$$

$$C_{FC_y} = CP_d FC_{DG} \tag{18}$$

$$C_{RE_y} = \sum_G 0.8 N_G PR_G \tag{19}$$

$$C_{SA_y} = -\sum_G 0.8 \left(1 - DE_G\right) N_G PR_G \tag{20}$$

where, G is the set of the four DERs, N_G is the quantity of each G, and CP_G is the capital price of DER in USD/unit. Also, OM_{DG} is the cost of O&M of DG in USD/h, OH_{DG} is the time of operation of the DG in hours, and OM_G is the cost of O&M of each G in USD/unit, and OM_G is the cost of O&M of each G in USD/unit. CP_d is the price of diesel fuel in USD/L and FC_{DG} is the DG fuel consumption in L. DE_G is the percent of linear degradation of each G.

Note that the costs represented by Eqs. (16) to (20) are calculated annually, hence the subscript y. The following expression is used to convert the annual values to present values:

$$NPC = \sum_{y=1}^{5} \frac{F_y}{\left(1 + i_f\right)^y} \tag{21}$$

where, NPC is the present cost of a cash flow F_y in the year y at a real discount rate i_f. Note that F_y represents the sum of costs of Eqs. (16) to (20) in the year y, and the replacement costs only exist when equipment reaches the end of its useful life and salvage only occurs at year 5. Replacement and salvage costs are multiplied by a factor of 0.8 since not all initial investments must be replaced or resold.

4.2. Constrains

The design variables are subject to technical restrictions associated with the generators' power limits, the maximum and minimum state of charge (SOC) of the BESS, and the desired reliability. This study did not consider the distribution system for simplicity; thus, the distribution losses are neglected. The capacity restrictions implemented were as follows:

$$N_G > 0 \tag{22}$$

$$\underline{P_{DG}} \leq P_{DG}(t) \leq \overline{P_{DG}} \tag{23}$$

$$\underline{P_{BESS}} \leq P_{BESS}(t) \leq \overline{P_{BESS}} \tag{24}$$

$$\underline{SOC} \leq SOC(t) \leq \overline{SOC} \tag{25}$$

$$SOC(t) = SOC(t-1) - P_{BESS}(t) \tag{26}$$

where, $P_{DG}(t)$ is the power delivered by the DG at time t in kW, and $\underline{P_{DG}}$ and $\overline{P_{DG}}$ are the minimum and maximum power delivered by the DG in kW, respectively. $\underline{P_{BESS}}$ and $\overline{P_{BESS}}$ are the maximum power delivered and absorbed by the BESS in kW, respectively. Finally, the state of charge $SOC(t)$ is limited by a minimum value $\underline{SOC}$ and a maximum value $\overline{SOC}$ and are expressed as a percentage.

In isolated MGs, it is usual that all the demand cannot be met all the time, so a reliability restriction is added. It is required that at least 95% of the demanded power is satisfied in all moments, so the Loss of Power Supply Probability (LPSP) was used as a reliability indicator:

$$LPSP = \frac{\sum_t IE(t)}{\sum_t P_L(t)} > 0.05 \tag{27}$$

where, $IE(t)$ is the insufficient energy at t time period (kWh) and $P_L(t)$ is the required load at t time period (kWh) [16]. A rule-based EMS was implemented to satisfy Eqs. (22) to (27), guaranteeing the load supply

and, thus, good reliability. The strategy is presented in the following subsection.

4.3. Rule-based energy management strategy

The rule-based EMS implemented allows taking full advantage of generation from renewable sources and optimizing DG and BESS dispatch considering their degradation. This strategy is executed once each hour during the time of the study (5 years). The sequence of actions of the strategy is following described:

1. The data corresponding to a possible solution is loaded, that is, the number of WT, PV, BESS, and DG.
2. The renewables generation is calculated from the models (see the following subsection).
3. The difference between generation with renewables and demand is calculated. For each instant interval t:
   - If the renewable generation is greater than the demand, the BESS is charged. The energy not supported by the BESS is computed as dump energy.
   - If the renewable generation is less than the demand, the power of the BESS and the DG is dispatched to minimize the cost of energy and degradation.
   - If the BESS and DG maximum capacities are not enough to meet the demand, the output power of this equipment is set to its maximum, and then an unattended load is computed.
4. Once the iterative EMS process is finished, the reliability indicators, emissions, and costs of the possible solution are calculated.
5. The next possible solution goes through the previous loop until all combinations are computed.

4.4. Modeling of the DERs

This subsection presents the models that allow converting primary resources to output power for renewable sources, the model used for BESS, and the relationship between power demanded by the DG and its fuel consumption.

4.4.1. Wind turbine

The calculation of the power generated by the WTs was made according to the wind speed. The model is described as [17]:

$$P_{WT}(t) = \begin{cases} P_R\left(\frac{V(t)^3 - V_{C_{in}}^3}{V_R^3 - V_{C_{in}}^3}\right) & V_{C_{in}} \le V < V_R \\ P_R & V_R \le V < V_{c_{out}} \\ 0 & \text{Otherwise} \end{cases} \quad (28)$$

where, P_R is rated power of the wind system, V_R is the rated speed of the WT in m/s, $V(t)$, $V_{C_{in}}$ and $V_{C_{out}}$ are the wind speed at instant t, the lower cutting speed, and the upper cutting speed in m/s, respectively.

4.4.2. Photovoltaic system

The chosen model is a simplified model presented by [17] to calculate the power output as follows:

$$P_{PV}(t) = N_{PV}\eta_{PV}A_{PV}I(t) \times \left(1 + \frac{k_p}{100}(T_c(t) - T_{STC})\right) \quad (29)$$

where, $P_{PV}(t)$, $I(t)$, and $T_c(t)$ represent the power generated in kW, the solar irradiance in kW/m^2, and the operating temperature in °C at an instant t. η_{PV}, A_{PV}, k_p, and T_{STC} are parameters that represent the efficiency, the effective area in m^2, the temperature constant in 1/°C, and the STC temperature of the panel in °C, respectively.

4.4.3. Battery energy storage system

As inferred from EMS, the battery power input/output depends on their SOC, power limits, and the EMS operation stage. Thus, the BESS can operate as follows:

- **Excess of renewables.** If the generation produced by renewable sources exceeds the demand, the excess charges the BESS. This power injection is limited by the SOC and the maximum battery charging power. If the BESS capacity is full, then Total Energy Lost (TEL) is computed.

$$P_{BESS}(t) = -(P_{WT}(t) + P_{FV}(t) - P_L(t)) \quad (30)$$

- **Defect of renewables.** If the generation of renewables is insufficient to satisfy the demand in an instant t, the BESS and DG are dispatched, minimizing the cost of generation. The cost of generating with BESS (C_{BESS}) is associated with their degradation, as follows:

$$C_{BESS}(t) = \frac{CP_{BESS}}{ETP_{BESS}}P_B(t), \; P_B(t) > 0 \quad (31)$$

where CP_{BESS} is the capital price in USD, and ETP_{BESS} is the energy throughput of the BESS in kWh. This equation assigns a fee to the kWh delivered by the battery considering its useful life in terms of energy. This cost is not considered within the C_{OM} or C_{FC} component since it is within the C_{SA} and C_{RE} calculation.

4.4.4. Diesel generation

Similarly to BESS, DG dispatch depends on EMS. The fuel consumption is used to calculate the cost of its operation and the component C_{FC}. The linear cost function of fuel consumption chosen is

$$FC_{DG}(t) = 0.246P_{DG}(t) + 0.08415NC_{DG} \quad (32)$$

where NC_{DG} is the nominal capacity of the DG in kW [46]. For dispatch purposes, an additional factor that includes degradation due to use was included. The dispatch cost function for the DG is

$$C_{DG}(t) = CP_{DG}FC_{DG} + \frac{CP_{DG}}{GE_{DG}}P_{DG}(t) \quad (33)$$

where, GE_{DG} is the total guaranteed energy that the DG can deliver during its entire useful life.

4.5. Study data

This section presents the primary resource associated with the case study presented. The MG sizing was made for an isolated location in the north of Colombia, in La Guajira (12.154°N, 72.063°W), since it has abundant solar and wind resources [47].

4.5.1. Load profile

The load profile was generated from typical residential profiles in Colombia. The highest demand occurs at the beginning of the night (18:00 to 20:00) and is equal to 20 kW, on average. In order to deal with the uncertainties introduced by the load consumption and meteorological data forecast, and the failure or maintenance events, the load profile must include a reliability factor that oversizes the consumption. For this work a factor of 1.2 was considered. Also, the profile contains a random variability of 15%.

4.5.2. Primary energy resources

Energy resources are the climatic variables that affect renewable generation. For this work, solar irradiance, wind speed, and ambient temperature are considered. These data were obtained from the EU Science Hub. Fig. 5 shows two days of the period of analysis in order to exemplify part of the data and show some typical values of the solar irradiance profile, wind speed, and temperature.

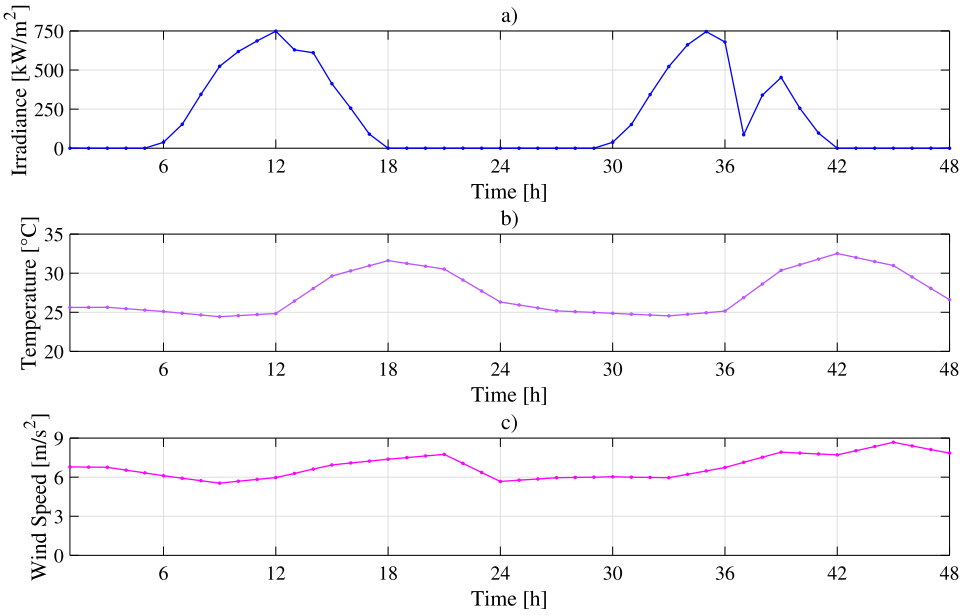

Fig. 5. Primary energy resources profiles. (a) Solar irradiance, (b) ambient temperature and (c) wind speed for 48 h.

Table 6
Economic parameters for system specification.

Parameter	Value	Unit	Parameter	Value	Unit
PR_{DG}	5000	USD/unit	OM_{WT}	450	USD/unit/yr
PR_{WT}	40 000	USD/unit	OM_{PV}	10.21	USD/unit/yr
PR_{PV}	714	USD/unit	OM_{BESS}	147	USD/unit/yr
PR_{BESS}	3057	USD/unit	i_f	6.59	%
OM_{DG}	0.17	USD/h	PR_d	0.79	USD/L

Table 7
Technical parameters for system specification.

Parameter	Value	Unit	Parameter	Value	Unit
C_{in}	3	m/s	$\underline{SOC}$	40	%
C_{out}	20	m/s	$\overline{SOC}$	100	%
CN_{WT}	10	kW	$\underline{P_{BESS}}$	−3	kW
V_R	10	m/s	$\overline{P_{BESS}}$	5	kW
η_{PV}	0.18	–	CN_{BESS}	9.80	kWh
A_{PV}	1.94	m^2	ETP_{BESS}	30 000	kWh
k_p	−0.35	–	LT_{DG}	15 000	h
T_{STC}	25	°C	GE_{DG}	63 750	kWh
CN_{PV}	0.34	kW	CN_{DG}	5	kW

4.5.3. Parameters

Parameters are divided into two categories: economic and technical parameters. The economic parameters are the values required for the cost calculations and are summarized in Table 6. Data associated with the mathematical models of the DER and constraints are presented in Table 7.

4.6. Solution method

It was used the parallel computing toolbox of Matlab software to solve the problem. The search space comprised 405,720 combinations and the limits are 0 to 160 PVs, 0 to 20 WTs, 1 to 30 BESS and 1 to 4 DGs. The total solution time was less than 8 min on a PC with an Intel (R) Core ™ i7-3770 CPU @ 3.40 GHz Quadra-core.

5. Results and discussion

This section presents the simulations and the discussion about their results and main findings. First, the results of the sizing formulation based on the proposed LCA approach are discussed. Then, these are confronted with a formulation that only considers the GWP impact, analyzing the underestimation of the environmental evaluation. Finally, the environmental component of the Pareto front solutions is presented and analyzed.

5.1. Proposed LCA approach

Once the sizing problem has been formulated and all the sizing combinations in the search space simulated, the Pareto Front is obtained. This is presented in blue in Fig. 6. Two solutions stand out from the figure according to the design criteria. An *Economical Solution* (EcS) which has the lowest cost of the front, and an *Environmental Solution* (EnS), which has the lowest environmental impact of the front. Table 8 summarizes the performance indicators of the solutions, including the composition of the MG sizing and the cost, reliability, and environmental indicators.

The EcS solution is located at the extreme left of the Pareto front since the x-axis corresponds to the cost. In contrast, the EnS is located at the bottom of the Pareto front since the y-axis corresponds to the environmental impact. In both cases, it is desirable to minimize each design criterion. This Pareto front corroborates the opposite relationship between economic and environmental objectives: a cost reduction implies a higher environmental impact. As expected, the solution must include more renewable sources and less diesel generation to reduce the environmental impact. For example, EcS includes 42 PVs, while EnS has 68 PVs more, for a total of 110 PVs. Also, the EnS has a 92% reduction in fuel consumption. Due to the price of renewables, this implies growth in costs. In this case, the EnS has a 60% higher cost in exchange for a 65% lower environmental impact.

Another key aspect of the results obtained is the values of the reliability indicators. EnS stands out for its high value in TEL (more than eight times higher than EcS), which is related to the high percentage of renewable generation production. Thus, the decrease in the use of diesel produces fewer environmental impacts but leads to more wasted energy.

5.2. Proposed LCA approach vs. GWP approach

The analysis of the underestimation of the environmental evaluation was done by comparing the proposed approach with an MG sizing

Table 8
Performance indicators for EcS, EcS-GWP, EnS and EnS-GWP of the sizing problem.

Composition	EcS				EcS-GWP				EnS				EnS-GWP			
	C_{FV}	C_{WT}	C_{DG}	C_{BS}	C_{FV}	C_{WT}	C_{DG}	C_{BS}	C_{FV}	C_{WT}	C_{DG}	C_{BS}	C_{FV}	C_{WT}	C_{DG}	C_{BS}
	42	1	2	3	42	1	2	3	110	2	1	30	48	4	1	30
NPC [USD]	99 016				99 016				158 100				172 808			
ESI [spe.-year]	9.20e−4				4.18e−4				3.19e−4				1.79e−4			
LPSP [%]	3.90				3.90				1.29				4.60			
TEL [%]	6.33				6.33				51.52				58.91			
Fuel consumed [L]	45 064				45 064				3448				9395			
FRA. OF REN. [%]	62.76				62.76				98.10				94.86			

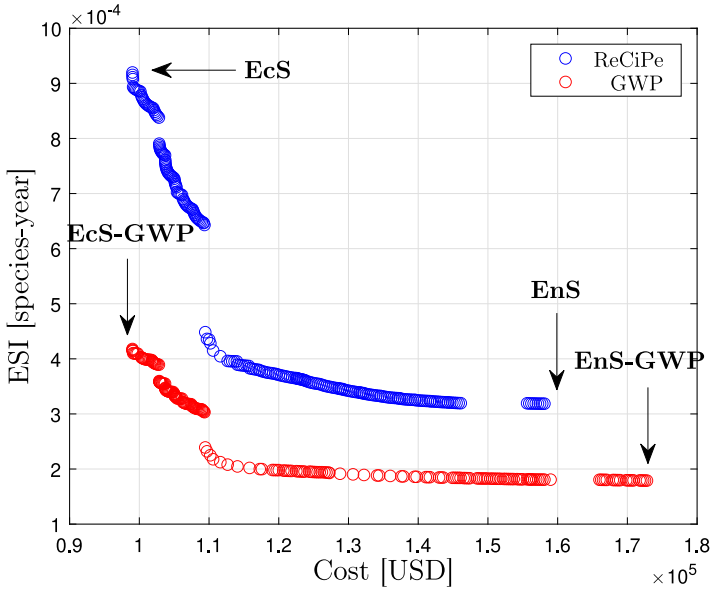

Fig. 6. Comparison between Pareto fronts considering ReCiPe and considering GWP.

approach that generalizes the common features of the state-of-the-art proposals (environmental impacts evaluated by exclusively calculating GWP in operation). Again, an *Economical Solution* and an *Environmental Solution* were calculated, denominated for this common approach EcS-GWP and EnS-GWP, respectively. The Pareto front of this approach is presented in red in Fig. 6, and the performance indicators are included in Table 8.

In Fig. 6, it is possible to observe that the Pareto front of the GWP approach presents lower values of the environmental impact, which is reflected in the covered ESI range covered. However, no significant variations are observed in the cost range of the solutions. For example, EcS and EcS-GWP presented the same configuration, but the ESI is 54.60% lower in EcS-GWP than EcS due to the underestimation of other environmental factors.

Regarding the environmental solutions, Table 8 shows that EnS-GWP presents an ESI 43.88% lower than EnS. Note that both approaches have different configurations (i.e., different quantities of DERs and ESS). EnS-GWP includes 56.3% fewer PVs than EnS, replacing this type of power generation with twice of WTs. This difference shows that the ESI is not a linear function of the configuration of the MG. For this reason, the solution considering only GWP is not necessarily the same as the proposed approach. In fact, EnS-GWP has a higher cost of implementation than EnS and is, in total, a more polluting sizing configuration. This can be observed in the total fuel consumed (2.7 times higher for EnS-GWP than EnS) and the fraction of renewables. Thus, an important aspect that can be concluded is that with a comprehensive analysis of environmental impacts, it is possible to make a better selection of the configuration of renewable generators in terms of the LC of the elements of the MG.

5.3. Composition of environmental impact on the Pareto front

In this subsection, the solutions of the Pareto front for the proposed LCA approach are presented in two stacked bar graphs, where it is shown the composition of its total environmental impact according to the impact category (Fig. 7(a)) and according to the DER technology (Fig. 7(b)). Note that the x-axis represents each of the solutions belonging to the Pareto front, stacked and organized from the lowest to highest NPC (highest to lowest ESI).

In Fig. 7(a), the quantification of GWP is shown in dark blue. Although this component is relevant in all solutions, it can be seen that in many of them, the sum of the rest of the impacts even exceeds the GWP. Mainly, FAET (purple) and AP (red) are essential components in environmental evaluation, and their quantification depends on the configuration of the MG and the percentage of renewables. For example, the solutions that are between 0 and 80 (the least expensive) are characterized by an important contribution of diesel generation (all include at least 2 DGs), which significantly increases FAET. After solution 80, a step in the figure is appreciated since all the solutions from this value onwards only have 1 DG. These solutions are more expensive, but a clear reduction in FAET is observed.

Fig. 7(b) allows to complement this analysis, showing the contribution by type of DER to the ESI. It is observed how, in the less expensive solutions, diesel generators contribute more than 70% of the environmental impact. For less polluting solutions, PV becomes the primary energy source, also becoming the source with more contribution to ESI. Regarding BESS, these devices increase their participation in ESI in more expensive configurations, in which the increase in PVs requires more batteries to ensure MG reliability. Finally, regarding WTs, this type of generation has a reduced contribution of ESI in almost all the

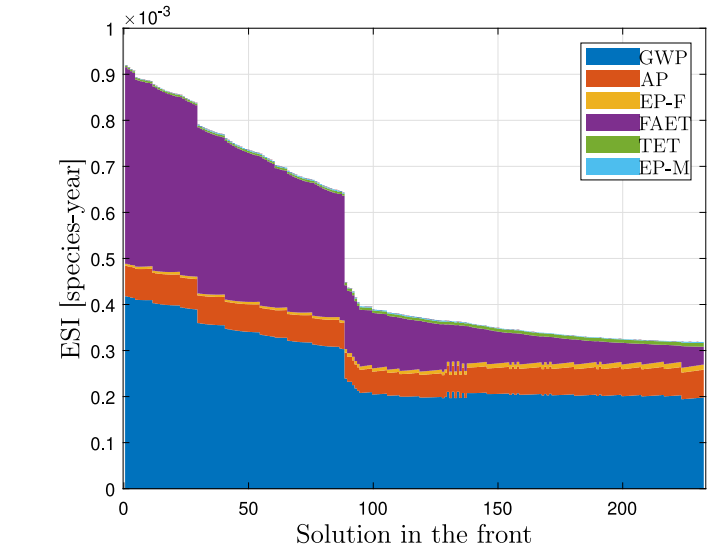

(a)

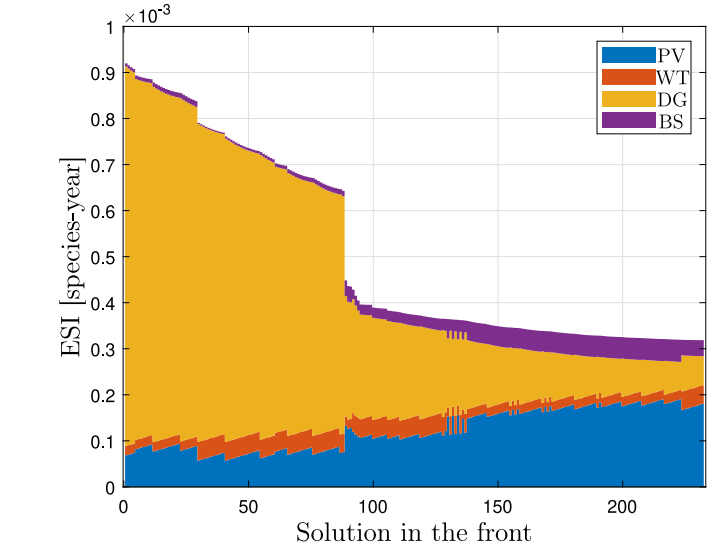

(b)

Fig. 7. Pareto front solutions with environmental impact discriminated by: (a) type of impact and (b) the impact of each DER technology.

solutions, with a strong relationship with AP, an indicator that also presents a low and homogeneous contribution to ESI in all the solutions shown in the figure.

6. Conclusions

This article presented an MG sizing approach that integrates the LCA based on the ReCiPe methodology. Unlike previous works that focus exclusively on the level of emissions of the MG operation, the proposal allows evaluating of the environmental impact in the main stages of an MG design, avoiding the underestimation of the environmental indicators. For this purpose, information from several sources was compiled to adapt LCA standardized methodologies in order to build an objective function into a techno-economic-environmental sizing formulation.

A case study of a solar/wind/battery/diesel microgrid is presented. The results allow to conclude the following aspects:

- The Pareto front corroborates the opposite relationship of the economic and environmental objectives. As expected, to reduce the environmental impact, the solution must include more renewable sources and less diesel generation, which implies significant cost growth. In the study case, the Environmental Solution (lowest environmental impact) has a 60% higher cost than the Economical Solution (lowest cost) in exchange for a 65% less environmental impact. Regarding the fraction of renewable energy, the Environmental Solution has 35% more than the Economical Solution.
- When the environmental impact was calculated considering only emissions in the microgrid operation, a value 54.60% lower was obtained than with the proposed approach. The indicators with the most significant impact on this difference are FAET and AP. Indeed, in many of the solutions, these components exceed the GWP.
- The underestimation of environmental indicators can lead to differences in the selection of the microgrid configuration. As an example, the configuration of the Environmental Solution considering only emissions in operation is different from the one

obtained with the proposed approach. In fact, the former is more expensive and polluting than the latter.

Future works will analyze the environmental impact of more types of DERs and ESSs, grid-connected MGs, and multi-MGs distributed systems. Also, other international LCA methodologies can be compared and/or integrated to assess the impact of MGs from various perspectives.

CRediT authorship contribution statement

Iván Jiménez-Vargas: Conceptualization, Methodology, Software, Validation, Formal analysis, Investigation, Data curation, Writing – original draft, Writing – review & editing, Project administration. **Juan M. Rey:** Conceptualization, Methodology, Software, Validation, Formal analysis, Investigation, Data curation, Writing – original draft, Writing – review & editing, Supervision. **German Osma-Pinto:** Data curation, Writing – review & editing, Supervision.

Declaration of competing interest

This research was funded by Universidad Industrial de Santander, project No. 2829-2021. The authors declare that they have no known competing financial interests or personal relationships that could have appeared to influence the work reported in this paper.

Data availability

Data will be made available on request.

References

[1] IEA, Global Energy & CO2 Status Report: Emissions, Technical Report, International Energy Agency, 2019, p. 14, URL: https://www.iea.org/geco/emissions/.

[2] G. Aydin, The modeling and projection of primary energy consumption by the sources, Energy Sources B 10 (1) (2014) 67–74, http://dx.doi.org/10.1080/15567249.2013.771716.

[3] G. Aydin, Regression models for forecasting global oil production, Pet. Sci. Technol. 33 (21–22) (2015) 1822–1828, http://dx.doi.org/10.1080/10916466.2015.1101474.

[4] S. Bahrami, A. Mohammadi, Smart Microgrids, first ed., Springer, Routledge, Abingdon, Oxon ; New York, NY, 2019, http://dx.doi.org/10.1007/978-3-030-02656-1, 2018.

[5] M. Farrokhabadi, C.A. Cañizares, J.W. Simpson-Porco, E. Nasr, L. Fan, P.A. Mendoza-Araya, R. Tonkoski, U. Tamrakar, N. Hatziargyriou, D. Lagos, R.W. Wies, M. Paolone, M. Liserre, L. Meegahapola, M. Kabalan, A.H. Hajimiragha, D. Peralta, M.A. Elizondo, K.P. Schneider, F.K. Tuffner, J. Reilly, Microgrid stability definitions, analysis, and examples, IEEE Trans. Power Syst. 35 (1) (2020) 13–29, http://dx.doi.org/10.1109/TPWRS.2019.2925703.

[6] A. Hirsch, Y. Parag, J. Guerrero, Microgrids: A review of technologies, key drivers, and outstanding issues, Renew. Sustain. Energy Rev. 90 (2018) 402–411, http://dx.doi.org/10.1016/J.RSER.2018.03.040.

[7] J.M. Rey, G.A. Vera, P. Acevedo-Rueda, J. Solano, M.A. Mantilla, J. Llanos, D. Sáez, A review of microgrids in Latin America: Laboratories and test systems, IEEE Latin Am. Trans. 20 (6) (2022) 1000–1011, http://dx.doi.org/10.1109/TLA.2022.9757743.

[8] R. Luna-Rubio, M. Trejo-Perea, D. Vargas-Vázquez, G.J. Ríos-Moreno, Optimal sizing of renewable hybrids energy systems: A review of methodologies, Sol. Energy 86 (4) (2012) 1077–1088, http://dx.doi.org/10.1016/j.solener.2011.10.016.

[9] S. Parhizi, H. Lotfi, A. Khodaei, S. Bahramirad, State of the art in research on microgrids: A review, IEEE Access 3 (2015) 890–925, http://dx.doi.org/10.1109/ACCESS.2015.2443119.

[10] M.D. Al-falahi, S.D. Jayasinghe, H. Enshaei, A review on recent size optimization methodologies for standalone solar and wind hybrid renewable energy system, Energy Convers. Manage. 143 (2017) 252–274, http://dx.doi.org/10.1016/j.enconman.2017.04.019.

[11] A. Ghasemi, M. Enayatzare, Optimal energy management of a renewable-based isolated microgrid with pumped-storage unit and demand response, Renew. Energy 123 (2018) 460–474, http://dx.doi.org/10.1016/j.renene.2018.02.072.

[12] J.M. Aberilla, A. Gallego-Schmid, L. Stamford, A. Azapagic, Design and environmental sustainability assessment of small-scale off-grid energy systems for remote rural communities, Appl. Energy 258 (November 2019) (2020) 114004, http://dx.doi.org/10.1016/j.apenergy.2019.114004.

[13] R. Poudel, J. Manwell, J. McGowan, Performance analysis of hybrid micro-hydro power systems, Energy Convers. Manage. 215 (2020) 112873, http://dx.doi.org/10.1016/j.enconman.2020.112873, URL: https://linkinghub.elsevier.com/retrieve/pii/S0196890420304118.

[14] H. Shamachurn, Optimization of an off-grid domestic Hybrid Energy System in suburban Paris using iHOGA software, Renew. Energy Focus 37 (2021) 36–49, http://dx.doi.org/10.1016/j.ref.2021.02.004, URL: https://linkinghub.elsevier.com/retrieve/pii/S1755008421000168.

[15] J.M. Rey, P.P. Vergara, J. Solano, G. Ordóñez, Design and optimal sizing of microgrids, in: Microgrids Design and Implementation, Springer, 2019, pp. 337–367, http://dx.doi.org/10.1016/j.solener.2019.06.050.

[16] J. Lian, Y. Zhang, C. Ma, Y. Yang, E. Chaima, A review on recent sizing methodologies of hybrid renewable energy systems, Energy Convers. Manage. 199 (August) (2019) 112027, http://dx.doi.org/10.1016/j.enconman.2019.112027.

[17] A.L. Bukar, C.W. Tan, K.Y. Lau, Optimal sizing of an autonomous photovoltaic/wind/battery/diesel generator microgrid using grasshopper optimization algorithm, Sol. Energy 188 (June) (2019) 685–696, http://dx.doi.org/10.1016/j.solener.2019.06.050.

[18] Y. Ali Shaabani, A.R. Seifi, M.J. Kouhanjani, Stochastic multi-objective optimization of combined heat and power economic/emission dispatch, Energy 141 (2017) 1892–1904, http://dx.doi.org/10.1016/j.energy.2017.11.124.

[19] T. Niknam, R. Azizipanah-Abarghooee, M.R. Narimani, An efficient scenario-based stochastic programming framework for multi-objective optimal micro-grid operation, Appl. Energy 99 (2012) 455–470, http://dx.doi.org/10.1016/j.apenergy.2012.04.017.

[20] S.R. Tito, T.T. Lie, T.N. Anderson, Optimal sizing of a wind-photovoltaic-battery hybrid renewable energy system considering socio-demographic factors, Sol. Energy 136 (2016) 525–532, http://dx.doi.org/10.1016/j.solener.2016.07.036.

[21] B. Dey, S.K. Roy, B. Bhattacharyya, Solving multi-objective economic emission dispatch of a renewable integrated microgrid using latest bio-inspired algorithms, Eng. Sci. Technol. Int. J. 22 (1) (2019) 55–66, http://dx.doi.org/10.1016/j.jestch.2018.10.001.

[22] E.E. Elattar, Modified harmony search algorithm for combined economic emission dispatch of microgrid incorporating renewable sources, Energy 159 (2018) 496–507, http://dx.doi.org/10.1016/j.energy.2018.06.137.

[23] D. Zhang, S. Evangelisti, P. Lettieri, L.G. Papageorgiou, Economic and environmental scheduling of smart homes with microgrid: DER operation and electrical tasks, Energy Convers. Manage. 110 (2016) 113–124, http://dx.doi.org/10.1016/j.enconman.2015.11.056.

[24] F. Asdrubali, G. Baldinelli, F. D'Alessandro, F. Scrucca, Life cycle assessment of electricity production from renewable energies: Review and results harmonization, Renew. Sustain. Energy Rev. 42 (2015) 1113–1122, http://dx.doi.org/10.1016/j.rser.2014.10.082.

[25] D.O. Akinyele, R.K. Rayudu, Techno-economic and life cycle environmental performance analyses of a solar photovoltaic microgrid system for developing countries, Energy 109 (2016) 160–179, http://dx.doi.org/10.1016/j.energy.2016.04.061.

[26] A. Petrillo, F. De Felice, E. Jannelli, C. Autorino, M. Minutillo, A.L. Lavadera, Life cycle assessment (LCA) and life cycle cost (LCC) analysis model for a stand-alone hybrid renewable energy system, Renew. Energy 95 (2016) 337–355, http://dx.doi.org/10.1016/j.renene.2016.04.027.

[27] H. Karunathilake, K. Hewage, W. Mérida, R. Sadiq, Renewable energy selection for net-zero energy communities: Life cycle based decision making under uncertainty, Renew. Energy 130 (2019) 558–573, http://dx.doi.org/10.1016/j.renene.2018.06.086.

[28] E. Bakhtavar, T. Prabatha, H. Karunathilake, R. Sadiq, K. Hewage, Assessment of renewable energy-based strategies for net-zero energy communities: A planning model using multi-objective goal programming, J. Clean. Prod. 272 (2020) 122886, http://dx.doi.org/10.1016/j.jclepro.2020.122886.

[29] P. Nagapurkar, J.D. Smith, Techno-economic optimization and environmental Life Cycle Assessment (LCA) of microgrids located in the US using genetic algorithm, Energy Convers. Manage. 181 (September 2018) (2019) 272–291, http://dx.doi.org/10.1016/j.enconman.2018.11.072.

[30] R. Nuvvula, E. Devaraj, K.T. Srinivasa, A comprehensive assessment of large-scale battery integrated hybrid renewable energy system to improve sustainability of a smart city, Energy Sources A (2021) 1–22, http://dx.doi.org/10.1080/15567036.2021.1905109.

[31] B. Shi, W. Wu, L. Yan, Size optimization of stand-alone PV/wind/diesel hybrid power generation systems, J. Taiwan Inst. Chem. Eng. 73 (2017) 93–101, http://dx.doi.org/10.1016/j.jtice.2016.07.047, URL: https://linkinghub.elsevier.com/retrieve/pii/S1876107016302905.

[32] T.M. Layadi, G. Champenois, M. Mostefai, Modeling and design optimization of an autonomous multisource system under a permanent power-supply constraint, IEEE Trans. Sustain. Energy 6 (3) (2015) 872–880, http://dx.doi.org/10.1109/TSTE.2015.2408622.

[33] M.A.P. Mahmud, N. Huda, S.H. Farjana, C. Lang, Techno-economic operation and environmental life-cycle assessment of a solar PV-driven islanded microgrid, IEEE Access 7 (2019) 111828–111839, http://dx.doi.org/10.1109/ACCESS.2019.2927653.

[34] D. Caro, Carbon Footprint, second ed., Elsevier Inc., 2018, pp. 1–6, http://dx.doi.org/10.1016/B978-0-12-409548-9.10752-3.
[35] National Institute for Public Health and the Environment, ReCiPe 2016 v1.1, Technical Report, National Institute for Public Health and the Environment, 2017, p. 201, URL: www.rivm.nl/en.
[36] M.I. Vega, C.A. Zaror, The Effect of Solar Energy on the Environmental Profile of Electricity Generation in Chile: A Midterm Scenario, Int. J. Energy Prod. Manag. 3 (2) (2018) 110–121, http://dx.doi.org/10.2495/EQ-V3-N2-110-121.
[37] B. Mendecka, L. Lombardi, Life cycle environmental impacts of wind energy technologies: A review of simplified models and harmonization of the results, Renew. Sustain. Energy Rev. 111 (April) (2019) 462–480, http://dx.doi.org/10.1016/j.rser.2019.05.019.
[38] A. Arvesen, E.G. Hertwich, Assessing the life cycle environmental impacts of wind power: A review of present knowledge and research needs, Renew. Sustain. Energy Rev. 16 (8) (2012) 5994–6006, http://dx.doi.org/10.1016/j.rser.2012.06.023.
[39] A.I. Stan, M. Swierczynski, D.I. Stroe, R. Teodorescu, S.J. Andreasen, Lithium ion battery chemistries from renewable energy storage to automotive and back-up power applications - An overview, in: 2014 International Conference on Optimization of Electrical and Electronic Equipment, OPTIM 2014, 2014, pp. 713–720, http://dx.doi.org/10.1109/OPTIM.2014.6850936.
[40] X. Sun, X. Luo, Z. Zhang, F. Meng, J. Yang, Life cycle assessment of lithium nickel cobalt manganese oxide (NCM) batteries for electric passenger vehicles, J. Clean. Prod. 273 (2020) 123006, http://dx.doi.org/10.1016/j.jclepro.2020.123006.
[41] K. Benton, X. Yang, Z. Wang, Life cycle energy assessment of a standby diesel generator set, J. Clean. Prod. 149 (2017) 265–274, http://dx.doi.org/10.1016/j.jclepro.2017.02.082, URL: https://linkinghub.elsevier.com/retrieve/pii/S0959652617302962.
[42] K. Sothea, N.T. Kim Oanh, Characterization of emissions from diesel backup generators in Cambodia, Atmos. Pollut. Res. 10 (2) (2019) 345–354, http://dx.doi.org/10.1016/j.apr.2018.09.001.
[43] Environment Canada, Greenhouse Gas Emissions and Criteria Air Contaminants, 2017, URL: https://www.canada.ca/en/environment-climate-change/services/environmental-funding.
[44] M. Owsianiak, A. Laurent, A. Bjørn, M.Z. Hauschild, IMPACT 2002+, ReCiPe 2008 and ILCD's recommended practice for characterization modelling in life cycle impact assessment: A case study-based comparison, Int. J. Life Cycle Assess. 19 (5) (2014) 1007–1021, http://dx.doi.org/10.1007/s11367-014-0708-3.
[45] J.M. Rey, I. Jiménez-Vargas, P.P. Vergara, G. Osma-Pinto, J. Solano, Sizing of an autonomous microgrid considering droop control, Int. J. Electr. Power Energy Syst. 136 (2022) 107634.
[46] J.M. Lujano-Rojas, C. Monteiro, R. Dufo-López, J.L. Bernal-Agustín, Optimum load management strategy for wind/diesel/battery hybrid power systems, Renew. Energy 44 (2012) 288–295, http://dx.doi.org/10.1016/j.renene.2012.01.097, URL: https://linkinghub.elsevier.com/retrieve/pii/S0960148112001243.
[47] J. Pasqualino, C. Cabrera, M.V. Chamorro, The environmental impacts of eolic and solar energy implementation in the Colombian Caribe, Prospect 13 (2015) 68–75, http://dx.doi.org/10.15665/rp.v13i1.361.